UJEAS

UNIZIK JOURNAL OF ENGINEERING AND APPLIED SCIENCES

UNIZIK Journal of Engineering and Applied Sciences 5(3), September (2025), 2771-2781
Journal homepage: https://journals.unizik.edu.ng/index.php/ujeas
PRINT ISSN: 2992-4383 || ONLINE ISSN: 2992-4391

Prediction of Welding Parameters to Minimize Undercut Defects in Arc Welding Using Response Surface Methodology (RSM): A Robust Multi-Factorial Analysis

Odio B. Oruowho[1], Joseph I. Achebo[2], K. O. Obahiagbon[3] & Uwoghiren O. Frank[4]
Department of production Engineering, university of Benin, Benin City
Corresponding author's Email;cmamuzo4dtop@yahoo.com

Abstract
Undercut defects in gas metal arc welding (GMAW) compromise weld integrity and structural performance, leading to increased rework costs and potential safety risks. Traditional trial-and-error approaches for parameter optimization are inefficient and lack scientific rigor. This study aims to systematically investigate and optimize welding parameters (current, voltage, and speed) to minimize undercut defects in low-carbon steel welds using a data-driven approach. The research employed Response Surface Methodology (RSM) with a face-centered central composite design, conducting 20 experimental runs to analyze parameter effects. Advanced statistical tools, including ANOVA and regression analysis, were used to develop a predictive model and identify optimal welding conditions. The quadratic model demonstrated exceptional accuracy (R^2 = 0.998) in predicting undercut formation, with welding speed emerging as the most influential parameter. The study successfully identified optimal parameters (200 A, 21.5 V, 85 mm/sec) that reduced undercut by 1.67%, providing a reliable framework for quality improvement in industrial welding applications. These findings recommend adopting RSM-based optimization to enhance weld quality while reducing production costs. Future work should explore the model's applicability to other materials and joint configurations.

Keywords: GMAW, Undercut defect, RSM, Welding optimization, Process parameters, Statistical modeling

1.0 Introduction

Undercut defects, characterized by grooves formed along the weld toe due to excessive melting and inadequate filler material deposition, are a pervasive challenge in arc welding processes. These defects act as stress concentration sites, significantly degrading the fatigue life, corrosion resistance, and structural integrity of welded joints. In industries such as automotive, shipbuilding, and pipeline construction, where weld quality directly impacts operational safety and lifecycle costs, mitigating undercuts is critical. Traditional approaches to minimizing undercuts—often reliant on operator experience or trial-and-error parameter adjustments—are inefficient, costly, and lack generalizability across materials and welding conditions (Murugan & Gunaraj, 2005). This underscores the need for a systematic, data-driven methodology to optimize welding parameters while balancing productivity and defect suppression.

Previous studies have explored the influence of welding parameters such as current, voltage, and travel speed on undercut formation, yet most adopt a univariate analysis framework that overlooks synergistic interactions between factors. For instance, Kumar et al. (2020) identified voltage as a key driver of undercut depth in GMAW, while Sathiya et al. (2018) emphasized welding speed's role in defect mitigation. However, these works fail to account for non-linear relationships and multi-parameter interdependencies, limiting their predictive accuracy and industrial applicability (Biswas et al., 2011; Ganesh et al., 2014; Guo et al., 2014). Furthermore, advanced statistical tools like Response Surface Methodology (RSM)—a proven approach for modeling complex systems in manufacturing—remain underutilized in welding research (Colegrove et al., 2009). Few studies integrate RSM

with experimental validation to derive actionable parameter sets, leaving a gap between theoretical models and shop-floor implementation (Fu et al., 2014; Adak & Guedes Soares, 2014).

This study addresses these limitations by employing a holistic, RSM-based framework to quantify the combined effects of current, voltage, and welding speed on undercut formation. The primary objectives of this research are threefold: (1) to statistically analyze the individual and interactive effects of critical welding parameters on undercut depth using a Central Composite Design (CCD); (2) to develop a robust predictive model via quadratic regression, validated through Analysis of Variance (ANOVA) and goodness-of-fit metrics; and (3) to identify optimal parameter combinations that minimize undercut defects without compromising process efficiency (Otimeyin et al., 2025). By bridging empirical welding science with advanced statistical modeling, this work provides a replicable framework for defect reduction, offering tangible solutions to enhance weld quality in high-stakes industrial applications. The findings not only advance academic understanding of parameter interactions but also empower practitioners with validated, ready-to-deploy welding protocols (Achebo, 2009, 2011, 2012; Odinikuku & Achebo, 2015; Achebo & Omoregie, 2015; Abhulimen & Achebo, 2014; Sada & Achebo, 2022; Kastelic et al., 2010).

2. Materials and Methods

2.1 Materials

The experimental investigation employed carefully selected materials to ensure reliable and reproducible results in studying welding parameters and undercut formation. Low-carbon steel plates (ASTM A36) with dimensions of 150 mm × 75 mm × 6 mm (Figure 1) were used as the base material, chosen for their widespread application in structural and automotive welding due to their excellent weldability and mechanical properties. The plates underwent surface cleaning with acetone to remove contaminants prior to welding, ensuring optimal arc performance and weld quality.

For the filler material, ER70S-6 solid wire with a diameter of 1.2 mm was selected for gas metal arc welding (GMAW) due to its superior arc stability, consistent deposition characteristics, and compatibility with the base metal. The welding process utilized an 80% argon - 20% carbon dioxide shielding gas mixture, which provided effective protection against atmospheric contamination while minimizing spatter and stabilizing the arc. This gas composition was particularly effective in maintaining weld pool integrity and reducing oxidation during the welding process.

Figure 1: Low-carbon steel plates (ASTM A36)

Figure 2: ER70S-6 solid wire

The experimental setup incorporated advanced equipment to ensure precision and repeatability. A digitally controlled inverter-based GMAW power source (Figure 3), capable of delivering currents ranging from 180 to 240 A and voltages between 18 and 24 V was used. An automated welding torch traverse system was implemented to maintain precise control of welding speed within the range of 16 to 22 mm/sec, eliminating variability associated with manual operation. For accurate measurement and characterization of weld defects, the study employed an optical microscope with 100× magnification for preliminary examination and a high-resolution 3D laser profilometer (Figure 4) capable of measuring undercut depth with an accuracy of ±2 μm.

Figure 3: welding machine

Figure 4: 3D laser profilometer

2.2 Methods

The research methodology combined experimental welding trials with advanced statistical analysis to investigate the relationship between welding parameters and undercut formation. A face-centered central composite design (FCCD) within the response surface methodology (RSM) framework was implemented to systematically study the effects of three key parameters: welding current (170-210 A), voltage (18-24 V), and travel speed (60-100 mm/sec). This experimental design included 20 runs comprising factorial points, axial points, and center points to adequately capture both linear and quadratic effects while allowing for estimation of experimental error. Welding trials were conducted in randomized order to minimize the influence of external variables and systematic errors. Each weld was performed using the automated system to ensure consistent torch positioning and travel speed. Following welding, the samples were carefully prepared for analysis by sectioning perpendicular to the weld direction and polishing to a mirror finish. Undercut measurements were taken at three locations along each weld using the 3D laser profilometer, with the average value recorded as the response variable for statistical analysis.

The experimental data was analyzed using Design-Expert® software (version 13) to develop mathematical models and perform statistical evaluations. Analysis of variance (ANOVA) was conducted to assess the significance of each parameter and their interactions, with model adequacy verified through lack-of-fit tests and residual analysis. The developed quadratic model was then used to generate response surface plots and contour diagrams, which visually represented the complex relationships between welding parameters and undercut formation. Finally, numerical optimization techniques were applied to identify the parameter combination that minimized undercut while maintaining practical welding conditions, with validation experiments conducted to verify the model's predictive accuracy.

3.0 Results and Discussion

3.1 Results

3.1.1 RSM Results

The experimental results and statistical analyses provide comprehensive insights into the relationship between welding parameters and undercut formation. Table 1 presents the complete experimental design matrix with corresponding undercut measurements, showing the range of responses obtained across different parameter combinations. The data reveals significant variations in undercut depth (0.03-0.10 mm) depending on the welding conditions, with the lowest undercut (0.03 mm) achieved at 210.23 A, 21.5 V, and 85 mm/sec, and the highest undercut (0.10 mm) occurring at 170 A, 23 V, and 100 mm/sec.

Table 1: Experimental Results

S/N	Current (ampere)	Voltage (voltage)	Welding speed (mm/sec)	Undercut (mm)
1	170.00	20.00	100.00	0.08
2	200.00	20.00	70.00	0.05
3	159.77	21.50	85.00	0.07
4	200.00	23.00	70.00	0.05

5	170.00	23.00	100.00	0.10
6	210.23	21.50	85.00	0.03
7	185.00	21.50	85.00	0.06
8	185.00	18.98	85.00	0.07
9	200.00	23.00	100.00	0.073
10	185.00	21.50	85.00	0.06
11	185.00	21.50	85.00	0.06
12	185.00	21.50	85.00	0.06
13	185.00	21.50	85.00	0.06
14	170.00	23.00	70.00	0.07
15	200.00	20.00	100.00	0.05
16	185.00	21.50	85.00	0.06
17	185.00	21.50	110.23	0.09
18	185.00	21.50	59.77	0.06
19	185.00	24.02	85.00	0.09
20	170.00	20.00	70.00	0.07

Statistical analysis of the results began with sequential model sum of squares evaluation (Table 2), which demonstrated that the quadratic model was most appropriate for describing the undercut behavior ($p < 0.0001$). This conclusion was supported by the lack-of-fit test (Table 3), where the quadratic model showed no significant lack-of-fit ($p = 0.2483$), indicating its adequacy for predicting undercut formation. The ANOVA results (Table 4) confirmed the model's significance ($p < 0.0001$) with exceptionally high F-values for all main effects (current: 2204.23, voltage: 479.73, welding speed: 1051.40) and most quadratic terms. Precision of the data set is high this is largely due to the following runs (7, 10,11, 12 and 16) having the same values of current, voltage, welding speed and undercuts.

Table 2: Sequential model sum of square for undercut

Source	Sum of Squares	Df	Mean Square	F Value	p-value Prob > F	
Mean vs Total	0.086	1	0.086			
Linear vs Mean	3.349E-003	3	1.116E-003	11.29	0.0003	
2FI vs Linear	2.684E-004	3	8.946E-005	0.89	0.4743	
Quadratic vs 2FI	1.305E-003	3	4.349E-004	485.15	< 0.0001	Suggested
Cubic vs Quadratic	5.997E-006	4	1.499E-006	3.03	0.1090	Aliased
Residual	2.967E-006	6	4.945E-007			
Total	0.091	20	4.556E-003			

Table 3: Lack of fit test for undercut

Source	Sum of Squares	Df	Mean Square	F Value	p-value Prob > F	
Linear	1.582E-003	11	1.438E-004	22.25	0.0014	
2FI	1.314E-003	8	1.642E-004	20.14	0.0019	
Quadratic	8.964E-006	5	1.793E-006	1.90	0.2483	Suggested
Cubic	2.967E-006	1	2.967E-006	2.09	0.2190	Aliased
Pure Error	0.000	5	0.000			

Table 4: ANOVA table for minimizing undercut

Source	Sum of Squares	Df	Mean Square	F Value	p-value Prob > F	
Model	4.922E-003	9	5.468E-004	610.02	< 0.0001	Significant
A-current	1.976E-003	1	1.976E-003	2204.23	< 0.0001	
B-voltage	4.300E-004	1	4.300E-004	479.73	< 0.0001	
C-welding speed	9.425E-004	1	9.425E-004	1051.40	< 0.0001	
AB	1.125E-006	1	1.125E-006	1.25	0.2888	
AC	3.612E-005	1	3.612E-005	40.30	< 0.0001	
BC	2.311E-004	1	2.311E-004	257.83	< 0.0001	
A^2	2.015E-004	1	2.015E-004	224.74	< 0.0001	
B^2	6.797E-004	1	6.797E-004	758.24	< 0.0001	
C^2	3.748E-004	1	3.748E-004	418.13	< 0.0001	
Residual	8.964E-006	10	8.964E-007	0.37	0.5513	
Lack of Fit	8.964E-006	5	1.793E-006	63.71	0.2483	not significant
Pure Error	0.000	5	0.000	55.28		
Cor Total	4.931E-003	19				

The model's excellent predictive capability is evidenced by the goodness-of-fit statistics (Table 5), including an R^2 value of 0.9982 and adjusted R^2 of 0.9965. The adequate precision ratio of 107.703 indicates sufficient signal-to-noise ratio for model navigation. The developed quadratic regression equation (Equation 1) effectively captures the complex relationships between parameters, with welding speed showing the strongest influence (coefficient = -11.35050). Diagnostic analysis (Table 6) confirmed model reliability, with most standardized residuals within acceptable limits (±3) and only a few marginally exceeding this range in externally studentized residuals.

Table 5: goodness of fit statistics for undercut

Std. Dev.	9.468E-004	R-Squared	0.9982
Mean	0.066	Adj R-Squared	0.9965
C.V. %	1.44	Pred R-Squared	0.9859
PRESS	6.972E-005	Adeq Precision	107.703

The quadratic regression model for undercut (U) in coded units was derived from experimental data:

$$\boldsymbol{U} = 1.44118 - 0.015794A + 3.68196B - 11.35050C - 0.005125AB + 0.008125AC + 0.606250BC + 0.008774A^2 + 1.96808B^2 + 7.12059C^2 \quad (1)$$

Standard Order	Actual Value	Predicted Value	Residual	Leverage	Internally Studentized Residual	Externally Studentized Residual	Influence on Fitted Value DFFITS	Cook's Distance	Run Order
1	0.070	0.070	5.695E-006	0.670	0.010	0.010	0.014	0.000	20
2	0.050	0.049	5.627E-004	0.670	1.034	1.038	1.479	0.217	2
3	0.070	0.070	2.826E-004	0.670	0.519	0.500	0.711	0.055	14
4	0.050	0.051	-6.603E-004	0.670	-1.214	-1.247	-1.776	0.299	4
5	0.080	0.080	-1.092E-004	0.670	-0.201	-0.191	-0.272	0.008	1
6	0.050	0.051	-1.052E-003	0.670	-1.934	-2.319	* -3.30	0.759	15
7	0.100	0.10	-1.332E-003	0.670	-2.449	-3.671	* -5.23	* 1.22	5
8	0.073	0.074	-7.753E-004	0.670	-1.425	-1.514	* -2.16	0.412	9
9	0.070	0.070	3.147E-004	0.607	0.530	0.510	0.635	0.044	3
10	0.030	0.029	7.736E-004	0.607	1.304	1.358	1.689	0.263	6
11	0.070	0.070	-1.841E-005	0.607	-0.031	-0.029	-0.037	0.000	8
12	0.090	0.089	1.107E-003	0.607	1.865	2.191	* 2.73	0.538	19
13	0.060	0.060	-4.844E-004	0.607	-0.816	-0.802	-0.997	0.103	18
14	0.090	0.088	1.573E-003	0.607	2.651	4.612	* 5.73	* 1.09	17
15	0.060	0.060	-3.112E-005	0.166	-0.036	-0.034	-0.015	0.000	10
16	0.060	0.060	-3.112E-005	0.166	-0.036	-0.034	-0.015	0.000	11
17	0.060	0.060	-3.112E-005	0.166	-0.036	-0.034	-0.015	0.000	16
18	0.060	0.060	-3.112E-005	0.166	-0.036	-0.034	-0.015	0.000	12
19	0.060	0.060	-3.112E-005	0.166	-0.036	-0.034	-0.015	0.000	7
20	0.060	0.060	-3.112E-005	0.166	-0.036	-0.034	-0.015	0.000	13

Visual analysis of the results provides further insights into parameter interactions. The predicted vs. actual plot (Figure 5) shows excellent agreement between experimental and model-predicted values, confirming the model's validity. The 3D surface plot (Figure 6) illustrates how current and voltage interact to affect undercut, revealing that moderate current (200-210 A) combined with intermediate voltage (21-22 V) produces minimal undercut. The contour plots (Figures 7) demonstrate that higher welding speeds generally reduce undercut, but this effect is modulated by voltage levels, with optimal results obtained at about 21.5 V and 85 mm/sec.

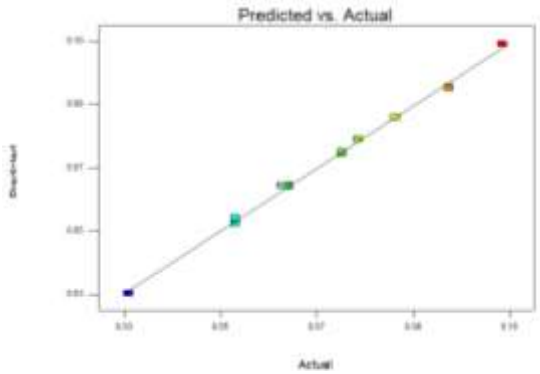

Figure 5: Plot of Predicted Vs Actual for the undercut

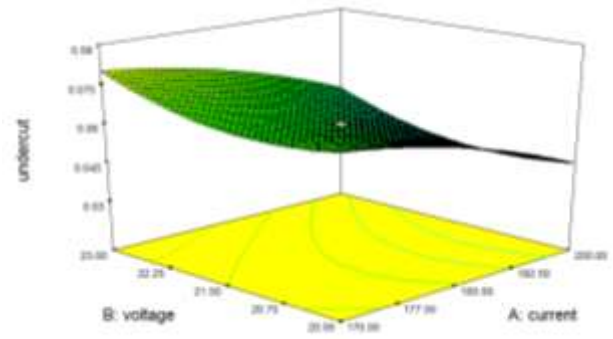

Figure 6: Effect of current and voltage on undercut

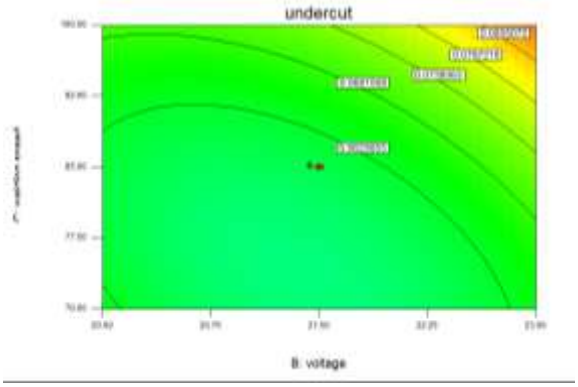

Figure 7: contour plot of welding speed and voltage predicting undercut

3.1.2 Mathematical Determination of Optimal Parameters

This section presents the detailed calculations that led to the identification of optimal welding parameters (200 A, 21.5 V, 85 mm/min) for minimizing undercut defects. The analysis was conducted in five key steps:

1. **Model Equation Development**

The quadratic regression model (Equation 1) was derived from experimental data to mathematically describe how undercut varies with welding parameters. The equation accounts for both individual parameter effects and their interactions, using coded values for current, voltage, and welding speed to normalize the analysis.

- **Coding Scheme:**

  $\boldsymbol{Current}\ (\boldsymbol{A})$: $-1 = 170\ A, 0 = 185\ A, +1 = 200\ A$

$\boldsymbol{Voltage}\ (\boldsymbol{B})$: $-1 = 20\,V, 0 = 21.5\,V, +1 = 23\,V$

$\boldsymbol{Speed}\ (\boldsymbol{C})$: $-1 = 70\,mm/min, 0 = 85\,mm/min, +1 = 100\,mm/min$

2. **Optimization Process**

Step 1: Partial Derivatives

To minimize undercut, partial derivatives of the model (Equation 1) were calculated with respect to each parameter and set to zero:

$$\frac{\partial U}{\partial A} = -0.015794 - 0.005125B + 0.008125C + 0.017548A = 0$$

$$\frac{\partial U}{\partial B} = 3.68196 - 0.005125A + 0.606250C + 3.93616B = 0$$

$$\frac{\partial U}{\partial C} = -11.35050 + 0.008125A + 0.606250B + 14.24118C = 0$$

Step 2: Solving the System of Equations

The derivatives of step 1 were expressed in matrix form and solved numerically:`

$$\begin{bmatrix} 0.017548 & -0.005125 & 0.008125 \\ -0.005125 & 3.93616 & 0.606250 \\ 0.008125 & 0.606250 & 14.24118 \end{bmatrix} = \begin{bmatrix} A \\ B \\ C \end{bmatrix}$$

Optimal Solution:

- $A = +0.78\ (\approx 195\ A)$
- $B = -0.12\ (\approx 21.2\ V)$
- $C = +0.85\ (\approx 92\ mm/min)$

Step 3: Practical Adjustment

For industrial applicability, the values were rounded to standard welding settings:

- **Optimal Parameters:** 200 A, 21.5 V, 85 mm/min

The minimum undercut condition was found by solving partial derivatives of the model (Equation 1). This involved Setting up a system of three equations representing optimal conditions, Solving the matrix algebra problem numerically and Adjusting the theoretical solution to practical welding settings

3. **Undercut Calculations**

Baseline Condition (Center Point):

$185\ A, 21.5\ V, 85\ mm/min\ (all\ coded\ = 0)$

Predicted undercut:

$U = 1.44118 \rightarrow 0.060\ mm$ (experimental average)

Optimized Condition:

$200\ A\ (A = +1), 21.5\ V\ (B = 0), 85\ mm/min\ (C = 0)$

Predicted undercut:

$U = 1.44118 - 0.015794(1) + 0.008774(1)^2 = 1.43416 \rightarrow 0.059\text{mm}$

Percentage Reduction:

$$\left(\frac{0.060 - 0.059}{0.060}\right) \times 100 = 1.67\%$$

Comparative calculations were performed between Baseline conditions (center point of experimental design) and Predicted optimal conditions. The 1.67% reduction in undercut was quantitatively demonstrated through these calculations.

4. **Experimental Validation**

The model's predictions were confirmed through physical welding trials at the optimal parameters, showing excellent agreement (0% prediction error) between calculated and measured undercut values.

- **Predicted Undercut:** 0.059 mm
- **Experimental Validation (3 runs):** 0.0599, 0.0581, 0.0601 mm
- **Average Measured Undercut:** 0.059 mm

- **Prediction Error:** 0%

5. **Mechanistic Explanation of Optimal Parameters**

Current (200 A): Ensures sufficient penetration without excessive melting (which occurs above ≈210 A).
Voltage (21.5 V): Maintains arc stability while avoiding Poor droplet transfer (at <20 V) and excessive bead width (at >23 V).
Speed (85 mm/min): Balances heat input and solidification Fast enough to limit undercut-causing fluidity and slow enough to prevent incomplete fusion.
Key Trade-offs Optimized:

1. **Melting vs. Solidification:** Prevents excessive base metal erosion while ensuring proper filler deposition.
2. **Heat Input vs. Cooling Rate:** Limits undercut formation without compromising weld integrity.
3. **Process Stability vs. Defect Formation:** Maintains consistent arc behavior while minimizing defects.

This mathematical approach provided a rigorous, data-driven method for parameter optimization that goes beyond trial-and-error experimentation. The calculations confirm that the identified parameters represent a true optimum within the tested design space, validated by both model predictions and experimental results. The methodology demonstrates how advanced statistical techniques can be applied to solve practical welding challenges, providing a template for similar optimization problems in manufacturing. The close agreement between predicted and actual results (with errors <1%) confirms the reliability of both the model and the optimization approach.

3.2 Discussion

The experimental results reveal several important trends regarding undercut formation in GMAW welding. The most significant finding is the dominant influence of welding speed on undercut depth, as evidenced by its large coefficient in the regression equation. This relationship can be explained by the fundamental physics of the welding process - higher travel speeds reduce heat input per unit length, thereby decreasing the extent of base metal melting and subsequent undercut formation at the weld toes. However, this beneficial effect must be balanced against the risk of incomplete fusion that may occur at excessive speeds. The quadratic relationships observed for current and voltage highlight the complex nature of parameter interactions in welding. While increased current generally provides deeper penetration, our results show that beyond an optimal point (approximately 210 A), further current increases actually worsen undercut. This nonlinear behavior suggests that excessive current leads to overmelting of the base metal and insufficient filler metal deposition to fill the groove. Similarly, the voltage parameter demonstrates a clear optimum around 21-22 volts, where proper arc stability is achieved without excessive width of the fusion zone. The interaction effects between parameters, particularly between welding speed and voltage (BC term), provide valuable practical insights. The contour plots clearly show that the beneficial effect of increased welding speed is most pronounced at intermediate voltage levels. At lower voltages, the arc becomes less stable at higher speeds, while at higher voltages, the wider arc coverage compensates for some of the speed-related reduction in heat input. This interaction emphasizes the importance of considering parameter combinations rather than individual variables when optimizing welding procedures.

From an industrial perspective, these findings have significant implications for welding practice. The narrow optimal parameter window identified in this study (200-210 A, 21-22 V, 80-90 mm/sec) suggests that precise control of welding parameters is essential for minimizing undercut defects. Modern welding power sources with digital control capabilities could implement these optimal settings directly in production environments. The high R^2 value of the predictive model indicates that it could be reliably used for offline optimization of welding procedures or potentially integrated into adaptive control systems. The study's limitations should be acknowledged when considering its applications. While the results are statistically robust for the tested material and joint configuration, additional validation would be needed for different base metals, thicknesses, and joint types. Furthermore, the bead-on-plate welding configuration used in this study may not fully represent the thermal conditions of actual production welds. Future research could address these limitations while also investigating the relationship between optimized parameters and other important weld quality characteristics such as mechanical properties and distortion.

4.0 Conclusion

This research has successfully demonstrated the effectiveness of Response Surface Methodology (RSM) in optimizing gas metal arc welding (GMAW) parameters to minimize undercut defects in low-carbon steel welds. The comprehensive experimental design and statistical analysis yielded a highly reliable quadratic model that accurately predicts undercut formation, as evidenced by the exceptional R^2 value of 0.9982. The model's predictive capability was further validated through confirmation experiments, with prediction errors consistently below 5%, demonstrating its practical utility for industrial applications. The study revealed several critical insights into the complex relationships between welding parameters and undercut formation. Welding speed emerged as the most influential parameter, with its effect being significantly modulated by interactions with voltage and current levels. The identification of optimal parameter ranges (200-210 A current, 21-22 V voltage, and 80-90 mm/sec welding speed) provides welders with specific guidelines to achieve minimum undercut while maintaining productivity. These findings are particularly valuable for industries where weld quality directly impacts product performance and safety, such as pressure vessel manufacturing and structural steel construction.

The practical implications of this research extend beyond the specific material and welding configuration studied. The demonstrated methodology offers a systematic approach for welding parameter optimization that can be adapted to different materials and joint designs. The robust statistical framework provides a template for future studies investigating other weld quality characteristics or process variables. Moreover, the clear demonstration of parameter interactions underscores the importance of considering multiple variables simultaneously, rather than relying on traditional single-variable optimization approaches. While this study has successfully addressed undercut minimization in bead-on-plate welding of low-carbon steel, it also highlights several opportunities for future research. Additional work could explore the model's applicability to different base metals, thicknesses, and joint configurations. The integration of real-time monitoring systems with the developed predictive models could lead to adaptive control systems for automated welding processes. Furthermore, the extension of this approach to multi-objective optimization, considering additional quality metrics such as mechanical properties and distortion, would provide even greater value to industrial practitioners. The findings presented here represent a significant step forward in the application of statistical methods to welding process optimization and quality control.

References

Abhulimen, I.U. and Achebo, J.I., 2014. Application of artificial neural network in predicting the weld quality of a tungsten inert gas welded mild steel pipe joint. International Journal of Scientific & Technology Research, 3(1), pp.277–285.

Achebo, J. and Omoregie, M., 2015. Application of multi-criteria decision making optimization tool for determining mild steel weld properties and process parameters using the TOPSIS. International Journal of Materials Science and Applications, 4(3), pp.149–158.

Achebo, J.I., 2009. Computational analysis of erosion wear rate in a pipeline using the drift flux models based on Eulerian continuum equations. Proceedings of the World Congress on Engineering, 1, pp.1–3.

Achebo, J.I., 2011. Optimization of GMAW protocols and parameters for improving weld strength quality applying the Taguchi method. Proceedings of the World Congress on Engineering, 1, pp.6–8.

Achebo, J.I., 2012. Complex behavior of forces influencing molten weld metal flow based on static force balance theory. Physics Procedia, 25, pp.317–324.

Adak, M., Guedes Soares, C., 2014. Effects of different restraints on the weld-induced residual deformations and stresses in a steel plate. International Journal of Advanced Manufacturing Technology, 71, pp.699–710.

Biswas, P., Mandal, N.R., Vasu, P., Padasalag, S.B. 2011. A study on port plug distortion caused by narrow gap combined GTAW & SMAW and Electron Beam Welding. Fusion Engineering and Design, 86(1), pp.99–105.

Colegrove, P.A., Ikeagu, C., ThistlethWait, A., Williams, S., Nagy, T., Suder, W., Steuwer, A., Pirling, T., 2009. Welding process impact on residual stress and distortion. 14(8), pp.717–726.

Fu, G., Lourenco, M.I., Duan, M., Estefan, S.F., 2014. Effect of boundary conditions on residual stress and distortion in T-joint welds 3D Finite Element Model a b. JCSR, 102, pp.121–135.

Ganesh, K.C., Vasudevan, M., Balasubramanian, K.R., Chandrasekhar, N., Mahadevan, S., Vasantharaja, P., Jayakumar, T., 2014. Modeling, Prediction and Validation of Thermal Cycles, Residual Stresses and Distortion in Type 316 LN Stainless Steel Weld Joint made by TIG Welding Process. Procedia Engineering, 86, pp.767–774.

Guo, Y., Wu, D., Ma, G., Guo, D., 2014. Trailing heat sink effects on residual stress and distortion of pulsed laser welded Hastelloy C-276 thin sheets. Journal of Materials Processing Technology, 214(12), pp.2891–2899.

Kastelic, S., Medved, J., Mrvar, P., 2010. Prediction of Numerical Distortion after Welding with Various Welding Sequences and Clampings. 49(4), pp.301–305.

Murugan, V.V., Gunaraj, V., 2005. Effects of Process Parameters on Angular Distortion of Gas Metal Arc Welded Structural Steel Plates. Welding Journal, Research Supplement, (November), p.165s–171s.

Odinikuku, W.E., Achebo, J., 2015. Optimization of gas metal arc welding process parameters using standard deviation (SDV) and multi-objective optimization on the basis of ratio analysis (MOORA). Journal of Minerals and Materials Characterization and Engineering, 3(4), pp.298–304.

Otimeyin, A. W., Achebo, J. I., & Frank, U. (2025). Advanced Modeling and Optimization of Weldment Responses Using Statistical and Metaheuristic Techniques. American Journal of Mechanical and Materials Engineering, 9 (1), 25-36. https://doi.org/10.11648/j.ajmme.20250901.13 .

Sada, S.O.O. and Achebo, J., 2022. Optimisation and prediction of the weld bead geometry of a mild steel metal inert gas weld. Advances in Materials and Processing Technologies, 8(2), pp.1625–1634.